Polysulfone based Membranes with Desired Pores Characteristics

DENISA (MANZU) FICAI*, ANTON FICAI, GEORGETA VOICU, BOGDAN STEFAN VASILE, CORNELIA GURAN, ECATERINA ANDRONESCU
Politehnica University of Bucharest, Faculty of Applied Chemistry and Material Science; 1-5 Polizu Str., 011061, Bucharest, Romania

Polysulfone based membranes with controlled porosity pore density, size and orientation were synthesized. The predicted pore characteristics are obtained by adding magnetite (nano or micro) particles into the polysulfone gel and the pores obtained by applying different magnetic fields. The pore density, size and orientation can be designed based on the magnetite particle concentration, on the magnetite particles size and respectively based on the angle between membrane surface and magnetite field. The pore density, size and orientation of the membranes were analyzed by SEM. FTIR was used to investigate the membrane composition and to prove the possibility of removing the magnetite particles by acidic dissolution or by extended membrane exposure to the magnetic field. The complex thermal analysis was used to characterize the thermal behaviour of the synthesized membranes.

Keywords: polysulfone membranes, pore characteristics, predicted porosity and separation ability, scanning electron microscopy

In the last years, separation membranes became essential materials not only in industries but also in daily human life [1-3]. Thus, separation membranes were used in many practical applications [4-6] including producing potable water from the seawater by reverse osmosis, recovering valuable constituents of solution by electrolysis, cleaning of industrial effluents, etc. Membranes have also been used to separate, remove, purify or partially recover individual components of gas mixtures, such as hydrogen, helium, carbon monoxide, carbon dioxide, oxygen, nitrogen, argon, methane and other light hydrocarbons. The membranes required for such applications are prepared from high polymers like polyimide, poly(amide–imide), polyphosphazene and polysulfone.

The separation ability of a membrane is dependent on its composition [7-12] and especially morphology [13, 14]. Membranes with controlled morphology can be used both in the separation process and chemical conversion, supplying highly ordered and confined geometries for chemical reactions [15, 16]. Even though such characteristics are continuously studied the knowledge in the field of pore design and preparation is still poor.

The most investigated and applied methods in the organic/inorganic membranes preparation are sol-gel [17-20], demixing processes [10, 21, 22], phase inversion by making up a polymeric ultra-thin layer [12, 23, 24], dry-wet spinning technique [25-27].

Magnetite particle have been used in many applications such as magnetic resonance imaging, drug delivery or hyperthermia supplier [28] but never to induce pore forming processes. Our purpose is to obtain membranes with predicted porosity (pore concentration, size and orientation) based on the interaction of magnetite particle with the applied magnetic field.

Experimental part

Materials

Polysulfone (BASF, ULTRASON®-S- 2010, fig. 1) was used as received. The polymer is conditioned as a white powder (d=1.24 g/cm^3) with low viscosity in organic solvents (50 mL/g, 25°C) and an average molecular weight of 40 000 Da.

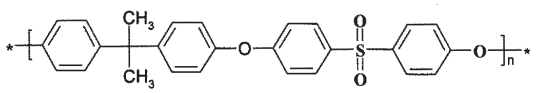

Fig. 1. Chemical structure of polysulfone ULTRASON®-S- 2010

Commercially available N–methylpirolidone (NMP) was used without further purification.

Equipment

The resulting membranes were investigated by Fourier transform infrared spectroscopy (FTIR) and scanning electron microscopy (SEM).

Infrared spectroscopy (IR) measurements were performed on a Vertex 70 instrument (Brucker) with Fourier transformation (FTIR), equipped with ATR module based on diamond crystal. The spectra were recorded over the wavenumber range of 400–4000cm^{-1} with a resolution of 2 cm^{-1} for all membranes.

SEM images were recorded on a HITACHI S2600N instrument with an EDS probe. Before imaging, all samples were covered with a thin gold layer.

The transmission electron images were obtained on finely powdered samples using a Tecnai™ G^2 F30 S-TWIN high resolution transmission electron microscope (HRTEM) equipped with STEM – HAADF detector, EDX and EELS. The microscope was operated in transmission mode at 300kV while TEM point resolution was 2Å and line resolution was 1 Å.

Methods

Polymer solution (15% wt) was obtained by starting from polysulfone and the corresponding volume of NMP in borosilicate glass vial with polyester caps followed by the solution filtration through a direct flow type module to remove any impurities.

The polysulfone membranes were obtained by applying the solution casting method. Casting of polymer solutions was performed by a doctor blade knife in a thin film of 0.4 mm on a glass plate. To obtain polysulfone membranes with desired pores characteristics, casting solutions were prepared from polysulfone solution and variable amount of magnetite particles followed by polymer solution casting

* email: manzu_denisa76@yahoo.com

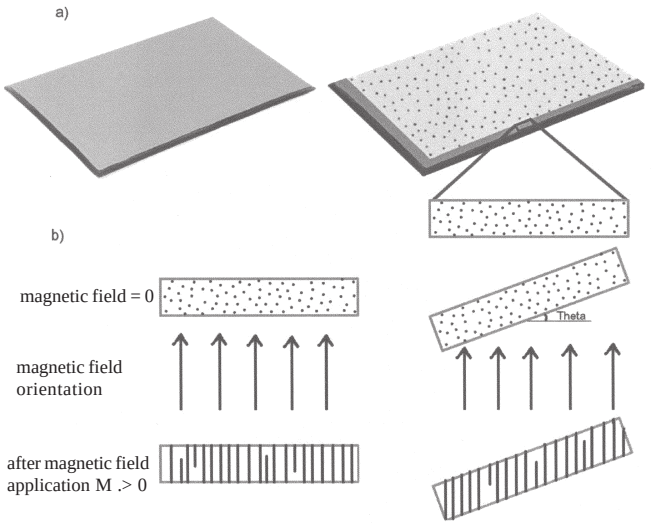

Fig. 2. Schematic representation of the controlled pore formation

(fig. 2a). The amount of particles added to the polymer solution was calculated based on the desired pore number per area to be obtained. The magnetite particles were obtained by co-precipitation from aqueous solution by starting from $FeSO_4$ and $FeCl_3$ as precursors at a *p*H of 9.

The magnetite particle removal can be achieved by two different methods: magnetic separation or acidic dissolution. Because of the lack of a higher magnetic field, the final removal of the magnetite particles was achieved by acidic dissolution.

A membrane of pure polysulfone solution was casted as a reference membrane (without addition of the magnetite particles).

A mixture of distilled water/solvent (the ratio being 2:8) was used as a coagulation agent at 25°C. During the coagulation process, a magnetic field of 500 mT was applied as shown in figure 2b. It is worth to mention that the pore length is a function of the theta angle while the pore density and size are not influenced by the magnetic field orientation.

In a membrane cross section the pore forming process is revealed in figure 2b.

Equation 1 describes quantitatively the membranes porosity based on the number of magnetite particles and membrane sizes.

The number of magnetite particles is in direct proportion with the added amount of magnetite and in inverse ratio with the magnetite particle size while the membrane area is in direct proportion with the amount of polysulfone based gel and gel concentration and in inverse ratio with the membrane thickness.

$$p = \frac{number\ of\ pores}{membrane\ area}\ [pores/\mu m^2]$$

Results and discussion

By phase-inversion process defect-free membranes with desired porosity were obtained. The characterization of the porous membranes was performed by Fourier transform infrared spectroscopy (FTIR), scanning electron microscopy (SEM) and complex thermal analysis (DTA-TG-DTG). The size and shape of the used magnetite nanoparticles were analyzed by TEM. For a better visualization the influence of magnetic field against the morphology of material, some adequate reference membranes were used as presented below.

Fourier transform infrared spectroscopy

After the polymer casting on the borosilicate glass and coagulation in the presence of the imposed magnetic field the membrane was analysed by FTIR (fig. 3a). Infrared spectroscopy was used especially to characterize the membrane materials and to appreciate the level of magnetite removal.

As the magnetic field application has not resulted in the magnetite removal entirely (the magnetite absorption bands are present: 877, 962, 1082, 1450 and 3686 cm^{-1}), additional acidic washing is mandatory. After washing, the IR spectrum of the membrane (fig. 3b) has revealed no magnetite absorption bands, proving that the magnetic particles were removed completely.

When the magnetite particle removal was achieved by dissolution in acid solution, the dissolution level was in direct proportion with the immersion time of the membrane in the acidic solution and in the inverse ratio with the *p*H.

By applying any of the two above-mentioned methods, the lack of the characteristic magnetite peaks has revealed the complete removal of magnetite.

The absorption bands of the material corresponds to the polysulfone groups, being in good agreement with standard polysulfone 1044cm^{-1} (SO_3H), 1106cm^{-1} (C-O), 1150cm^{-1} ($R(SO_2)$-R), 1241cm^{-1} (C-O), 1488cm^{-1} (aromatic bond), 2966cm^{-1} (aliphatic CH), 2879cm^{-1} (aromatic CH) and 3362cm^{-1} (OH).

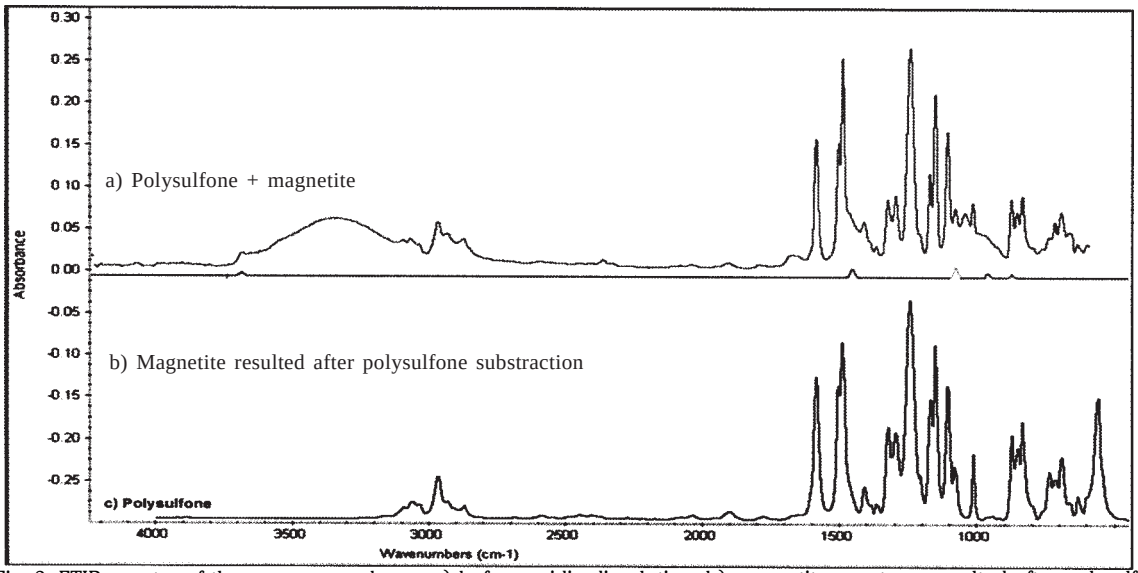

Fig. 3. FTIR spectra of the porous membrane a) before acidic dissolution, b) magnetite spectrum resulted after polysulfone subtraction and c) polysulfone spectrum after acidic dissolution of magnetite

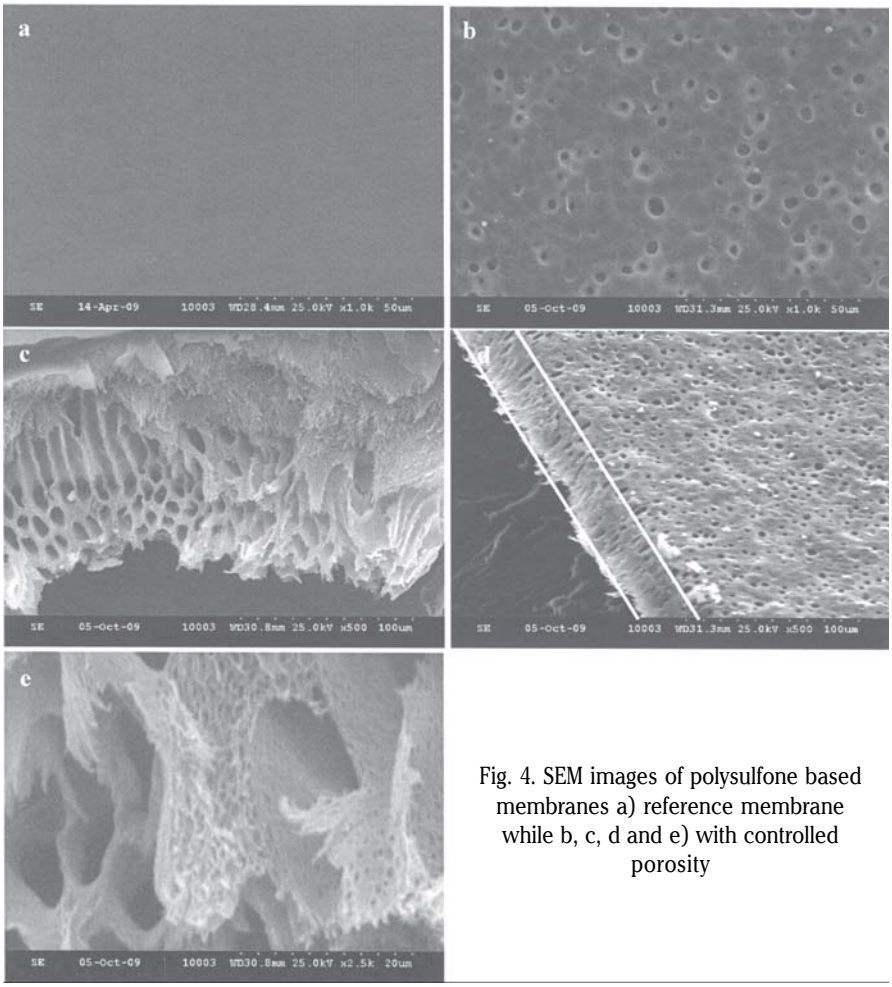

Fig. 4. SEM images of polysulfone based membranes a) reference membrane while b, c, d and e) with controlled porosity

Scanning electron microscopy

Scanning electron microscopy was employed to investigate the membrane morphology. Very suggestive from this point of view are the images presented in figure 4, especially 5a and b. The proposed methods can be seen to modify the membrane porosity, the pore sizes being approximately the same as the magnetite particle sizes. Because the used magnetite particles were agglomerated, the pore sizes reach up to 5 μm, such membranes being employable in the microfiltration.

In a cross section view at different magnifications (fig. 4c-e) the resulting pores can be analyzed. From the point of view of the pore sizes, a bimodal pore distribution can be identified: pores exceeding 5μm in diameter and pores of less than 1μm in diameter. The pores exceeding 5μm in diameter have resulted from the migration of the magnetite agglomerations while the pores of less than 1μm in diameter have resulted from the migration of the magnetite particle.

The magnetite particle migration is influenced by the particle sizes, the smaller particle having the highest penetrating power. There are pores (especially large pores) which are not open on both faces of the membrane as revealed in figure 2. Two types of small pores can be identified: pores linking two large pores and pores linking the two faces of the membrane. At a higher magnification (fig. 4e), the membrane materials exhibit a uniform pore distribution of the narrow pores. The membrane open porosity estimated based on the equation 1 is ~ 1pore/ μm^2.

Complex thermal analysis

The thermal behaviour of the polysulfone membranes is very important for many applications. The main processes (fig. 5) which occur when polysulfone is heated are: solvent evaporation identified as an endothermic effect accompanied by mass loss at ~129^{0}C and the polysulfone degradation which occur in two stages (526 and 615 ^{0}C) accompanied by mass loss. The membrane thermal stability is very good and starts at temperature higher than 400^{0}C.

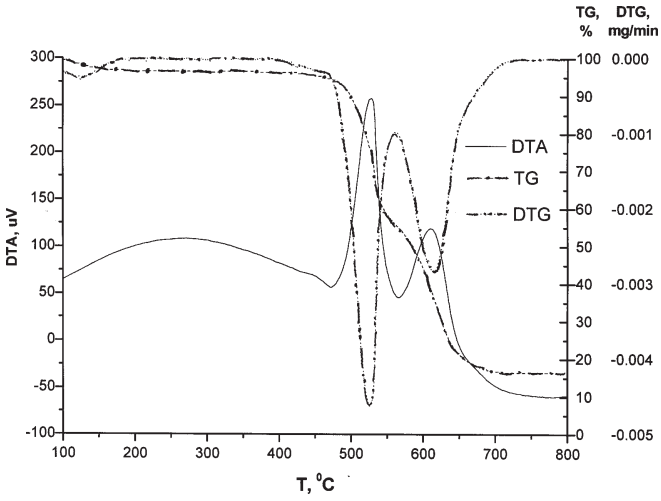

Fig. 5. Thermal behavior of polysulfone based membrane with desired pore characteristics

Transmission electron microscopy

Due to the nanoscale dimension of the magnetite particles, the transmission electron microscopy was used to characterize the magnetite nanoparticles. Based on the TEM images, it can be concluded that magnetite nanoparticles have predominantly spherical shape and the diameter of the particles is in the range of 1 – 50 nm. The

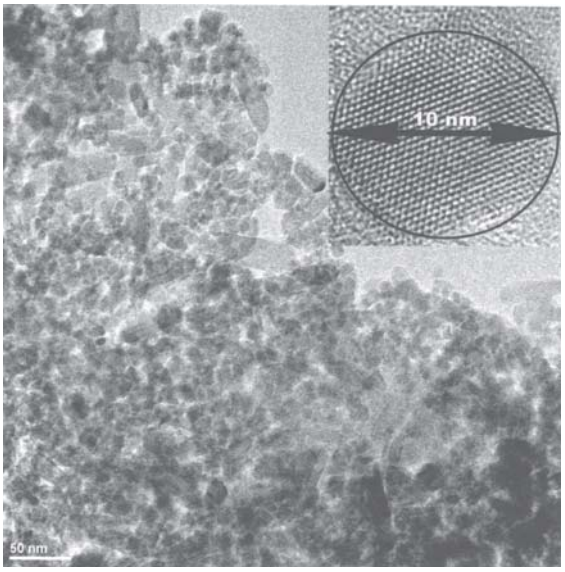

Fig. 6. TEM image of magnetite nanoparticles and the insert corresponds to HRTEM image of a characteristic magnetite nanoparticle of 10 nm diameter

average diameter of magnetite nanoparticles is about 20 nm.

Conclusions

The phase inversion method applied in preparing the polysulfone-based membrane was improved by the addition of magnetite particles followed by pore formation due to the application of the magnetic field. Due to the pore forming process, the resulting membrane morphology can be improved by classical phase inversion method.

The magnetic field influence on the magnetic particles is crucial in the pore forming process. The pores characteristics are dependent on the pore density (dependent on the magnetic particle concentration - in the starting gel), the pore sizes (in direct proportion with the particle sizes) while the pore orientation (referred to the membrane) - is dependent on the angle between the membrane plane and magnetic field vectors.

FTIR analyses have revealed the "pore forming process" to be a non-contaminant process, the used magnetite particles being removed entirely by acidic dissolution.

Acknowledgements: The authors would like to thank to National Authority for Scientific Research – ANCS and The National University Research Council – CNCSIS.

References

1. TWARDOWSKI, Z. J., Seminars in Dialysis, **19**, no. 3, 2006, p.217
2. ISLA, A., GASCON, A.R., MAYNAR, J., ARZUAGA, A., CORRAL, E., MARTIN, A., SOLINIS, M. A., MUNOZ, J.L.P., Clinical Therapeutics, **27**, no. 9, 2005, p.1444
3.KARIDURAGANAVAR, M. Y., NAGARALE, R. K., KITTUR, A. A., KULKARNI, S. S., Desalination, **197,** 2006, p.225
4. CAMACHO-ZUNIGA, C., RUIZ-TREVINO, F. A., HERNANDEZ-LOPEZ, S., ZOLOTUKHIN, M. G., MAURER, F. H. J., GONZALEZ-MONTIEL, A., Journal of Membrane Science, **340**, no. 1-2, 2009, p.221
5. GARGANCIUC, D., BATRINESCU, G., NECHIFOR, G., OLTEANU, M., Mat. Plast., **45**, no. 1, 2008, p.29
6. HAMCIUC, C. and HAMCIUC, E., Mat. Plast., **43,** no. 3, 2006, p.204
7. ARTHANAREESWARAN, G., THANIKAIVELAN, P., RAAJENTHIREN, M., Materials Science & Engineering C, **29**, no. 1, 2009, p.246
8. WU, H., FANG, X., ZHANG, X. F., JIANG, Z. Y., LI, B., MA, X. C., Separation and Purification Technology, **64**, no. 2, 2008, p.183
9. WENG, T. H., TSENG, H. H. and WEY, M. Y., International Journal of Hydrogen Energy, **33**, no. 15, 2008, p.4178
10. MOHAMMADI, T., KIKHAVANDI, T., MOGHBELI, M., Macromolecular Symposia, **264**, 2008, p.127
11. MADAENI, S.S., HOSEINI, S., Journal of Polymer Research, **16**, no. 5, 2009, p.591
12. WANG, B., HUANGFU, F., LIU, W., Journal of Applied Polymer Science, **108**, no.6, 2008, p.4014
13. YAVE, W., QUIJADA, R., Desalination, **228**(1-3), 2008, p.150
14. RAHIMPOUR, A., MADAENI, S. S., Journal of Membrane Science, **305**, no. 1-2, 2007, p.299
15. FONTANANOVA, E., DONATO, L., DRIOLI, E., LOPEZ, L., FAVIA, P., D'AGOSTINO, R., Chemistry of Materials, **18**, 2006, p.1561
16. BONCHIO, M., CARRARO, M., SCORRANO, G., FONTANANOVA, E., DRIOLI, E., Advanced Synthesis & Catalysis, **345,** 2003, p.1119
17. WIJAYA, S., DUKE, M. C., DA COSTA, J. C. D., Desalination, **236**, no. 1-3, 2009, p.291
18. BATTERSBY, S., TASAKI, T., SMART, S., LADEWIG, B., LIU, S. M., DUKE, M. C., RUDOLPH, V. , DA COSTA, J. C. D., Journal of Membrane Science, **329**, no. 1-2, 2009, p.91
19. AGOUDJIL, N., KERMADI, S., LARBOT, A., Desalination, **223**, no. 1-3, 2008, p.417
20. PAKIZEH, M., OMIDKHAH, M. R., ZARRINGHALAM, A., International Journal of Hydrogen Energy, **32**, no. 12, 2007, p.1825
21. HAN, M. J., BHATTACHARYYA, D., Journal of Membrane Science, **98**, no. 3, 1995, p.191
22. CHENG, L.P., YOUNG, T.H., CHUANG, W.Y., CHEN, L.Y., CHEN, L.W., Polymer, **42**, no. 2, 2001, p.443
23. QTAISHAT, M., KHAYET, M., MATSUURA, T., Journal of Membrane Science, **341**, no. 1-2, 2009, p.139
24. SIVAKUMAR, M., SUSITHRA, L., MOHAN, D. R., RANGARAJAN, R., Journal of Macromolecular Science Part a-Pure and Applied Chemistry, **43**, no. 10, 2006, p.1541
25. ZHU, S. J., BRANFORD-WHITE, C., ZHU, L.M., HE, C.J., WANG, Q.R., Desalination and Water Treatment-Science and Engineering, **1**, no. 1-3, 2009, p.201
26. ZHU, L. P., ZHU, B. K., XU, Y. Y., Journal of Applied Polymer Science, **101**, no. 2, 2006, p.878
27. LEE, S. H., KIM, J. J., KIM, S. S., KIM, U. Y., Journal of Applied Polymer Science, **49**, no. 3, 1993, p.539
28. ITO, A., SHINKAI, M., HONDA, H., KOBAYASHI, T., Journal of Bioscience and Bioengineering, **100**, no. 1, 2005, p.1

Manuscript received: 26.10.2009